

RESEARCH ARTICLE | MARCH 23 2023

# Effect of magnetic disorder on Cr interaction with $1/2\langle 111 \rangle$ screw dislocations in bcc iron

Luis Casillas-Trujillo  ; Björn Alling 



*Journal of Applied Physics* 133, 125103 (2023)

<https://doi.org/10.1063/5.0134935>



Export  
Citation

CrossMark

## Articles You May Be Interested In

Screw dislocation assisted martensitic transformation of a bcc Cu precipitate in bcc Fe

*Appl. Phys. Lett.* (January 2007)

Atomistic study of temperature dependence of interaction between screw dislocation and nanosized bcc Cu precipitate in bcc Fe

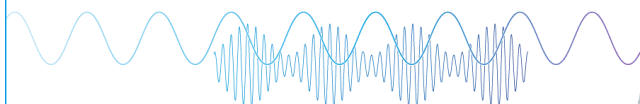
*Journal of Applied Physics* (October 2008)

Conceptual Design of the Topaz II Anticriticality Device

*AIP Conference Proceedings* (July 1994)

Webinar

Boost Your Signal-to-Noise  
Ratio with Lock-in Detection



Sep. 7th – Register now



Zurich  
Instruments

# Effect of magnetic disorder on Cr interaction with $1/2\langle 111 \rangle$ screw dislocations in bcc iron

Cite as: J. Appl. Phys. **133**, 125103 (2023); doi: [10.1063/5.0134935](https://doi.org/10.1063/5.0134935)

Submitted: 15 November 2022 · Accepted: 6 March 2023 ·

Published Online: 23 March 2023



Luis Casillas-Trujillo<sup>1,2,a)</sup> and Björn Alling<sup>2</sup>

## AFFILIATIONS

<sup>1</sup>Inorganic Chemistry, Department of Chemistry—Ångström Laboratory, Uppsala University, Uppsala, Sweden

<sup>2</sup>Department of Physics, Chemistry and Biology (IFM), Linköping University, Linköping 58183, Sweden

<sup>a)</sup>Author to whom correspondence should be addressed: [luis.casillas.trujillo@liu.se](mailto:luis.casillas.trujillo@liu.se)

## ABSTRACT

We investigate how the magnetic state influences the interaction of Cr substitutional impurities with  $1/2\langle 111 \rangle$  screw dislocations in bcc Fe via density functional theory (DFT). We compare the paramagnetic state, modeled with a non-collinear disordered local moment (DLM) model, with the ferromagnetic state. In a previous work [Casillas-Trujillo *et al.*, Phys. Rev. B **102**, 094420 (2020)], we have shown that the magnetic moment and atomic volume landscape around screw dislocations in the paramagnetic state of iron are substantially different from that in the ferromagnetic state. Such a difference can have an impact in the formation energies of substitutional impurities, in particular, magnetic solutes. We investigate the formation energies of Cr solutes as a function of position with respect to the screw dislocation core, the interaction of Cr atoms along the dislocation line, and the segregation profile of Cr with respect to the dislocation in paramagnetic and ferromagnetic bcc iron. Our results suggest that with increasing temperature and connected entropic effects, Cr atoms gradually increase their occupation of dislocation sites, close to twice the amount of Cr in the DLM case than in the ferromagnetic case, with possible relevance to understand mechanical properties at elevated temperatures in low-Cr ferritic steels in use as structural materials in nuclear energy applications.

© 2023 Author(s). All article content, except where otherwise noted, is licensed under a Creative Commons Attribution (CC BY) license (<http://creativecommons.org/licenses/by/4.0/>). <https://doi.org/10.1063/5.0134935>

## I. INTRODUCTION

Iron has been of great technological importance, even more its alloying with carbon that gave rise to steel and Cr that gave corrosion resistance. Iron alloys are used as structural materials in many applications, and steels with a low-Cr content have shown resistance to temper embrittlement<sup>1</sup> and to neutron radiation induced swelling;<sup>2–4</sup> therefore, they are currently the forefront candidates to be used as structural materials for nuclear fusion and next generation fission reactors.<sup>5,6</sup> As such, they are subjected to high operational temperatures. In these critical circumstances, reliability is a paramount aspect; structural materials must possess high mechanical stability;<sup>7</sup> thus, a fundamental understanding of the deformation mechanisms at high temperatures is needed.<sup>8</sup> The phenomena of dislocation nucleation and mobility are essential for understanding plastic deformation and macroscopic mechanical properties of materials. In particular, the plastic behavior in body centered cubic iron is attributed to screw dislocation core effects.<sup>9,10</sup> The segregation of solute atoms to or away from dislocation cores is a phenomenon central to solid-solution hardening. It is known that the

addition of solute atoms to a base metallic element may cause an increase or a decrease in the yield strength, which phenomenon is referred to as solid-solution hardening or softening, respectively. Solute atoms can impact the dislocation core structure.<sup>8,11–14</sup> Long-range interactions are dominated by elasticity, but elasticity fails to describe the core region where solutes might have a pronounced effect, as such *ab initio* calculations are suitable for dislocation core structure determination and interaction with point defects.<sup>10,15–17</sup>

One of the consequences of high temperature is an increase in magnetic disorder. Magnetic materials such as iron possess a spontaneous magnetization, but as the temperature increases, the magnetic moments start to become disordered until the critical temperature, in bcc Fe 1043 K, when the system no longer exhibits any long-range magnetic ordering, yet the local spin polarization of the atoms is still present and are often critical for mechanical properties.<sup>18</sup> It can be noted that diffusion in materials is higher at elevated temperatures while that typically distinctly suppressed at room temperature; furthermore, a dramatic change in the activation energy of diffusion near the Curie temperature occurs in  $\alpha$ -iron,

24 August 2023 13:41:05

meaning that atomic and defect structures can be determined in the high temperature paramagnetic state.<sup>19–21</sup>

Theoretical dislocation studies are computationally demanding, requiring large supercells or complex simulation setups, even more so including dislocations with magnetism.<sup>22–24</sup> Similarly, the simulation of magnetic disorder by first principle calculations is challenging and is sometimes mistakenly approximated by the non-magnetic state, but this approach leads to incorrect results<sup>25,26</sup> as has been demonstrated in several materials' systems.<sup>27–29</sup> The magnetic state has an impact on point defect formation energies, and recent studies in bcc iron have shown that there exists a difference in point defect formation energy between the ferromagnetic and paramagnetic regimes where a better agreement with the experimental results is obtained when the relevant magnetic state is chosen.<sup>27,29,30</sup> Thus, the magnetic state can alter the interaction of point defects with dislocations, leading to different segregation profiles.

The present paper investigates the effect of magnetic disorder on the energetics of Cr solute interactions with a dislocation in bcc iron. We have chosen Cr for its relevance in steels and for its known peculiar mixing behavior with Fe in the perfect bulk. In a previous study,<sup>31</sup> we have found that the magnetic moment and atomic volume landscapes in the paramagnetic state in bcc iron are substantially different from the ferromagnetic case. We investigate the effects of this difference on how solutes decorate the  $1/2\langle 111 \rangle$  screw dislocation core, and we compare and contrast their behavior in the paramagnetic and ferromagnetic states.

## II. METHODS

In order to describe the paramagnetic state, we employ the disordered local moment (DLM) approach.<sup>32</sup> The high temperature paramagnetic case can be viewed as a disordered distribution of local magnetic moments with no long-range order. In the DLM also, the short-range order (SRO) is approximated as zero, an approximation that is good far above the critical temperature. However, it is a robust limiting case that together with the knowledge of the ordered ferromagnetic state, brackets all real magnetic states with temperature-dependent SRO. The DLM approach allows us to formulate a consistent electronic structure based thermodynamic theory that accounts for the interplay between the configurational and magnetic degrees of freedom.<sup>33</sup> In the DLM simulations, the direction of the magnetic moments is assigned randomly and can be easily implemented in a supercell approach.<sup>18,34</sup>

To model screw dislocation with *ab initio* methods, we utilize a quadrupole periodic array of dislocation dipoles.<sup>17</sup> This approach allows the utilization of fully periodic boundary conditions and stable dislocations since the dislocation arrangement cancel the stress field to a first order.<sup>35</sup> The dislocation dipole is introduced into the simulation cell by applying the displacement field of each dislocation as given by anisotropic linear elasticity using the Babel code.<sup>36</sup> It has been shown that this methodology is able to obtain converged dislocation core structures and energies.<sup>15</sup>

The DFT calculations are performed using the projector augmented wave method<sup>37</sup> as implemented in the Vienna *Ab initio* Simulation Package (VASP)<sup>38,39</sup> with the Perdew–Burke–Ernzerhof generalized gradient approximation<sup>40</sup> to model the

exchange-correlation effects. Only the 4s and 3d electrons of Fe and Cr are treated as valence, while the remaining electrons are part of the PAW potentials. All calculations are performed using a 400 eV kinetic-energy cutoff, a Methfessel–Paxton 0.2 eV broadening, and with a convergence criterion on all forces of 0.01 eV/Å for structural relaxations. Introducing a Cr atom in the supercell creates a row of solute atoms along the  $[111]$  direction. To assess the Cr–Cr interaction, we used an 8b (8 Burgers vector) supercell with two Cr atoms. Assessing the Cr–Cr interaction by using a slab with one Cr atom and using its periodic images to assess the Cr–Cr interaction with different supercell sizes are problematic due to the different Cr concentrations of the supercells. From our 8b cell calculations, we found that 3b is a big enough supercell size for considering Cr atoms distant and used it for the DLM calculations. Calculations were performed on supercells with 405 and 1080 atoms using  $1 \times 2 \times 6$  and  $1 \times 2 \times 2$  *k*-point grids for the 3b and 8b-cells, respectively.

## III. RESULTS

### A. Relaxations in the DLM state

Geometric relaxations can have an important contribution on the formation energy of point defects. In the case of vacancies in bcc iron, a  $\sim 0.1$  eV difference in formation energy between the geometries obtained in the FM and in the paramagnetic state was found.<sup>27</sup> To relax structures in the magnetic disordered state is very costly in both computer and real time. This is because the magnetic disordered moments in real paramagnetic materials are dynamically fluctuating on a timescale much faster than the diffusion of atoms. This means that in calculations, it is not enough to relax a structure with one frozen disordered magnetic cell. Instead, the relaxation must be done taking many different magnetic configurations into account in a procedure modeling a real time-averaging process. Previously, we have obtained the relaxed screw dislocation structure in the DLM state of pure bcc Fe.<sup>31</sup> Introducing a Cr atom in the system will produce displacements to the atoms around it, being more pronounced on its nearest neighbors. We have analyzed the effect of relaxations due to the presence of a Cr solute in bulk bcc iron in the DLM state and in the dislocation system in the FM case. The relaxation methodology for the DLM state is described in Ref. 27 in which atoms are partially allowed to relax according to different disordered magnetic configurations in sequence until a steady displacement of the atoms from the initial positions is achieved. The equilibrium positions of each atom are obtained by averaging the atomic positions of several configurations once the relaxation is in the steady state. The convergence criteria and the displacements for the non-equivalent atomic positions in the supercells are shown in Fig. 1, with the largest displacement of 0.014 Å corresponding to the first nearest neighbors to the Cr atom. Since displacements are small, we do not perform explicit DLM relaxations when we add the Cr solute and start from the pure iron DLM relaxed dislocation structure. In the FM calculations, we compare both including and not including specific Cr-induced relaxations. In Fig. 3, we include the results for an unrelaxed and relaxed system with a Cr solute and observe that there is no qualitative change and only small effects on the quantitative energies that will not change the overall trends of the study.

24 August 2023 13:41:05

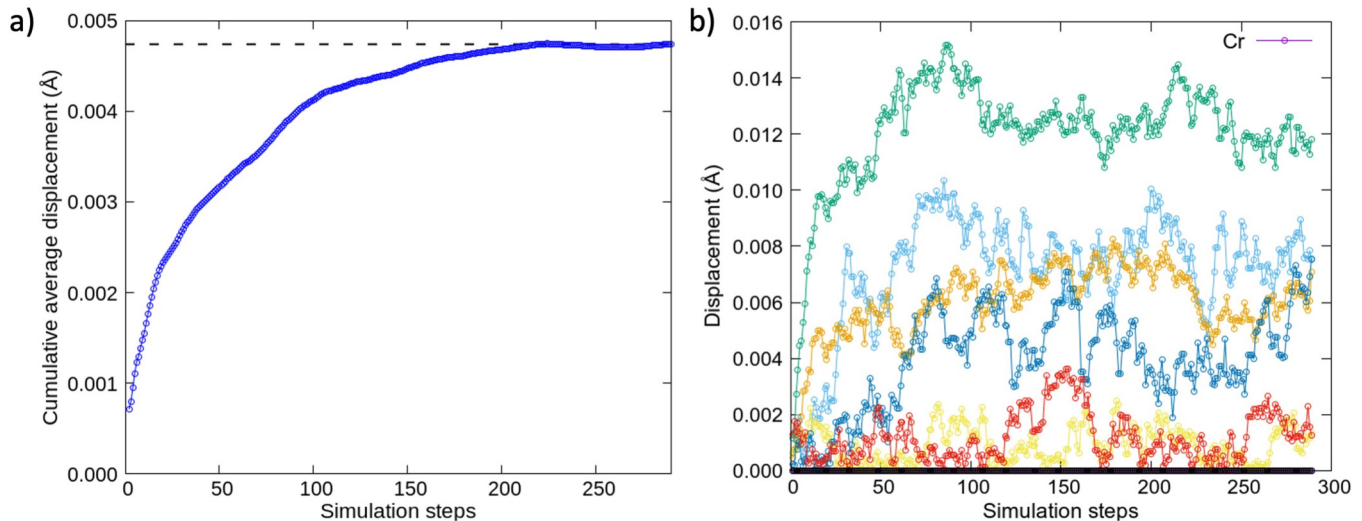


**FIG. 1.** (a) Cumulative average displacement as a function of simulation step number. (b) Cumulative displacement of the symmetrically distinct atomic positions in the supercell.

## B. Cr in bulk bcc iron

We assess the formation energies of Cr in bulk bcc iron (dislocation free) and compare between the ferromagnetic state and the DLM state. We have used a 128 atoms cubic supercell where we have introduced two Cr atoms with different separation distances along the [111] direction. The formation energies in the DLM case are obtained by averaging the results of 20 different magnetic configurations. For the formation energy, the reference states are DLM bcc Fe and nonmagnetic bcc Cr for the DLM case, since the latter is the magnetic result when we start with a DLM bcc Cr. For the alloys in the FM state, FM bcc Fe and AFM bcc Cr are the reference states. Using NM bcc Cr as the reference lowers the curve by 0.02 eV. From Fig. 2, it can be observed that in the FM case, Cr wants to be as far away as possible from other Cr atoms and their solution energy into Fe is negative favoring solubility. The magnetic moment direction of the Cr atoms is pointing in the opposite direction to Fe atoms. In the DLM state, the solution energy is positive. In addition, the lowest energy corresponds to the Cr atoms being next to each other, while the largest energy corresponds to the case where they are the farthest apart. The differences in formation energies as a function of Cr separation are, however, an order of magnitude lower than in the FM case. This suggests in any case a clustering tendency in the DLM case, opposite to the FM behavior. Fe–Cr alloys display strong solubility tendency also at low temperatures for concentrations below 6% Cr;<sup>41,42</sup> in this situation, Cr atoms like to be surrounded by Fe atoms. When the concentration increases, Cr atoms have to be close to each other and the mixing enthalpy becomes positive. In Fe–Cr alloys, it has been shown that the magnetic disorder removes the specific mixing trend with negative mixing enthalpy at a low-Cr content but also decreases the magnitude of the positive mixing enthalpy at a higher Cr content.<sup>27</sup> Our results are,

thus, fully in line with the previous findings for Cr-poor  $\text{Fe}_{1-x}\text{Cr}_x$  alloys in the defect free bcc bulk.

## C. Cr–Cr interaction along the dislocation line in FM iron

Next, we consider the case of a Cr impurity in a system containing dislocations in the ferromagnetic case. In this way, we assess the Cr–Cr interaction to determine the required cell size to approximate the dilute limit. We employ a supercell with 8b thickness to avoid comparing systems with different Cr concentrations. We use the easy core configuration since it has the lowest energy for both FM and disordered magnetic states in pure bcc Fe.<sup>31</sup> In contrast with interstitial carbon,<sup>14</sup> Cr does not lead to a dislocation core reconstruction from the easy to the hard core.<sup>7</sup> We placed the Cr in the position closest to the dislocation core. Figure 3 shows the energies and magnetic moment magnitudes for the different Cr–Cr separation distances along the [111] direction, where we have taken the largest separation Cr–Cr energy as a reference. From this, we conclude that a 3b supercell in thickness is a good choice for the dilute limit calculations.

## D. DLM calculations

Finally, we perform DLM calculations for the system containing the dislocations. Figure 4 shows the energies for a Cr solute as a function of distance to the dislocation core comparing the FM and disordered magnetic moments state. The solute–dislocation interaction energy per solute atom is defined as the energy difference between the case when the solute atom is in the dislocation core or infinitely separated from the dislocation core. In this sense, negative energies correspond to an attraction to the dislocation. In practice, in our case, we have set the reference energy as the farthest

24 August 2023 13:41:05

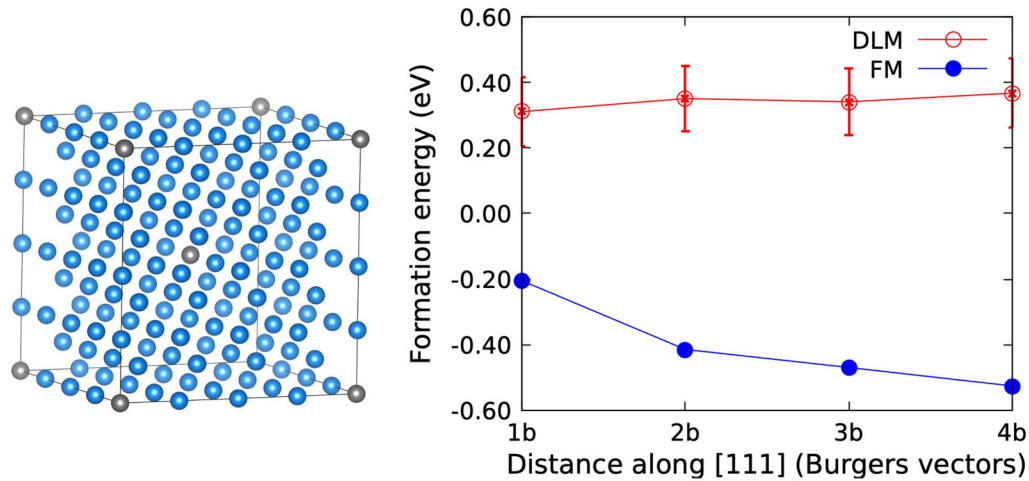


FIG. 2. Comparison of the formation energy of Cr substitutional impurities in bulk bcc iron in the ferromagnetic and DLM states.

possible position from the dislocation core in the supercell. For both FM and DLM states, Cr atoms have an energetic preference to avoid the dislocation core as the energy of the position furthest away from the core is the lowest. However, among the three considered dislocation sites close to the core, the energy is the lowest for the position closest to the dislocation core. The FM results are in agreement with the ones previously reported by Odbadrakh *et al.*<sup>7</sup> In the DLM calculations, approximating the paramagnetic state,

the energy difference between the sites is smaller, and the positive values of the dislocation core sites are lower in magnitude as compared to the FM calculations. Thus, the energetic preference to avoid the dislocation core seen in the FM case is still present in the DLM state but much weakened.

If we go into the details of our simulations and compare the individual different disordered magnetic configurations, they have a significant effect on the segregation profile energy value. To best

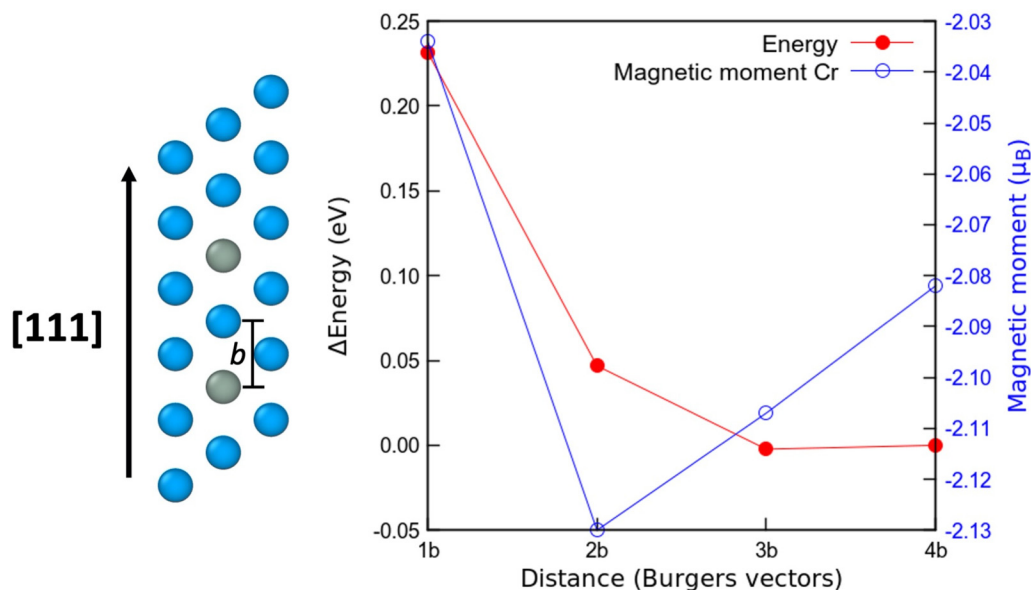
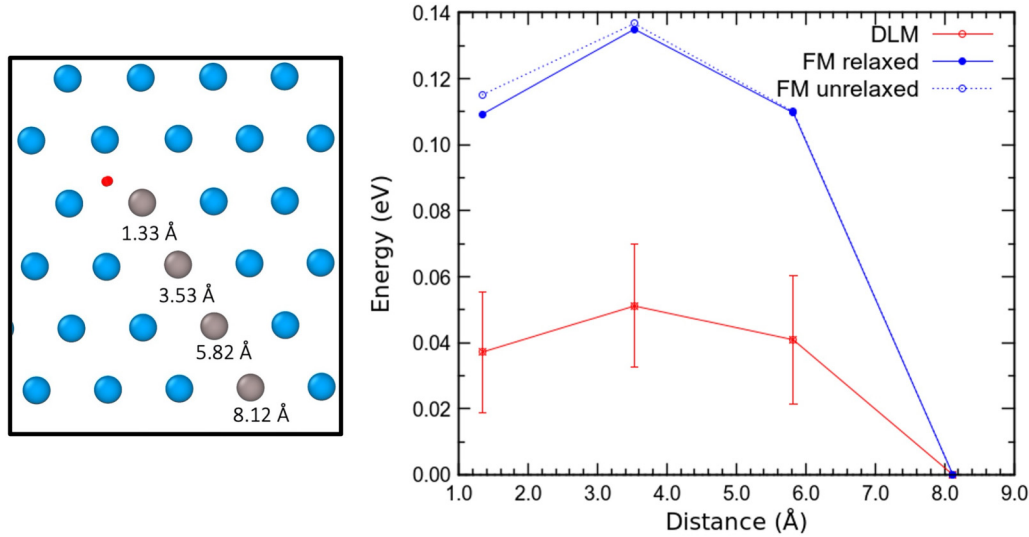


FIG. 3. Formation energy of Cr substitutional impurities in the presence of a dislocation for ferromagnetic bcc iron as a function of Cr–Cr distance along the [111] direction. Also shown are the Cr magnetic moments.

24 August 2023 13:41:05





**FIG. 4.** Energies of a Cr solute as a function of distance to the dislocation core in a 3b supercell. The red dot in the left image represents the screw dislocation line perpendicular to the page.

compare among the different Cr positions in the DLM state, we used the most similar magnetic configuration, and this means we used the same magnetic moment template for the different Cr positions and averaged over 40 different configuration templates. The error of the mean value  $P(\sigma_{\bar{p}})$ , shown as an error bar for the DLM curve in Fig. 4, is calculated as the standard error  $\pm 2\sigma_{\bar{p}} = 2\sigma_p/\sqrt{N}$  giving a confidence interval of 95%, where  $N$  is the number of employed configurations. We also assessed the clustering tendencies along the [111] direction in the DLM case using a supercell with  $4b$  thickness and calculating the energies for Cr atoms separated  $1b$  and  $2b$ , obtaining a value of  $E^{2b} - E^{1b} = 0.009$  eV, indicating, in contrast to the FM case, a very weak repulsion for Cr–Cr along the dislocation line. This further contributes to a larger possibility for Cr to occupy positions along the dislocation line in the DLM state as compared to the FM state.

### E. Segregation profile

Based on the energetic profiles obtained above, we can perform a mean-field analysis<sup>43,44</sup> to study the segregation tendencies of Cr to or from the dislocation core as a function of temperature. This is done using the methodology of Ventelon *et al.*,<sup>14</sup> which studied carbon interstitials in iron. This approximation accounts for configurational entropy but neglects local chemical environment effects, vibrational, and electronic entropy. We consider only nearest neighbor interactions between solute atoms. The concentration for a specific site close to the dislocation core  $C_d$  is given by

$$\frac{C_d}{1 - C_d} = \frac{C_{bulk}}{1 - C_{bulk}} \exp\left(-\frac{E_{seg}(C_d)}{k_B T}\right). \quad (1)$$

The segregation energy  $E_{seg}$  is given by

$$E_{seg}(C_d) = E_{int} + C_d \frac{\partial E_{int}}{\partial C_d} = E_{int}^0 + 2C_d V_{cc}, \quad (2)$$

where the interaction energy is defined as the energy difference between the case when the solute atom is in the dislocation core or infinitely separated from the dislocation, which is approximated by the farthest position from the core (see Fig. 4).  $V_{cc}$  is the first neighbor repulsion energy between solute atoms. The solute concentration is connected to nominal concentration  $C_{nom}$  by matter conservation,  $N_b C_{bulk} + N_d C_d = N_0 C_{nom}$ . The number of solute sites in the dislocation core is  $N_d = \rho V n / b$ , and the total number of sites  $N_0 = 2V/a^3$ , where  $\rho$  is the dislocation density,  $V$  is the volume of the system,  $a$  is the lattice constant,  $b$  is the Burgers vector, and  $n$  is the number of sites in the core. In Fig. 5, the segregation profile as a function of temperature for a system with 5% Cr is presented, modeled using our energetics from our dilute Cr modeling above. The analysis shows, that at low temperatures, there is little Cr content in the dislocation core since the solute–dislocation interaction is repulsive and Cr atoms would prefer to be in the bulk. Raising temperatures will allow for Cr to occupy dislocation sites due to entropic arguments. As an example, we can discuss 1000 K, which is close to the Curie temperature of Fe, at which one can see the FM and DLM states as bracketing the real magnetic state that should display an intermediate degree of short-range magnetic order. At 1000 K, the amount of Cr at the dislocation core calculated for the FM state is only about 25% of the bulk value, while the DLM calculations suggest a Cr concentration in the dislocation core of around 60% of the bulk value. This difference originates in the reduced repulsion by the dislocation in the DLM case, and the ability to cluster together along the dislocation

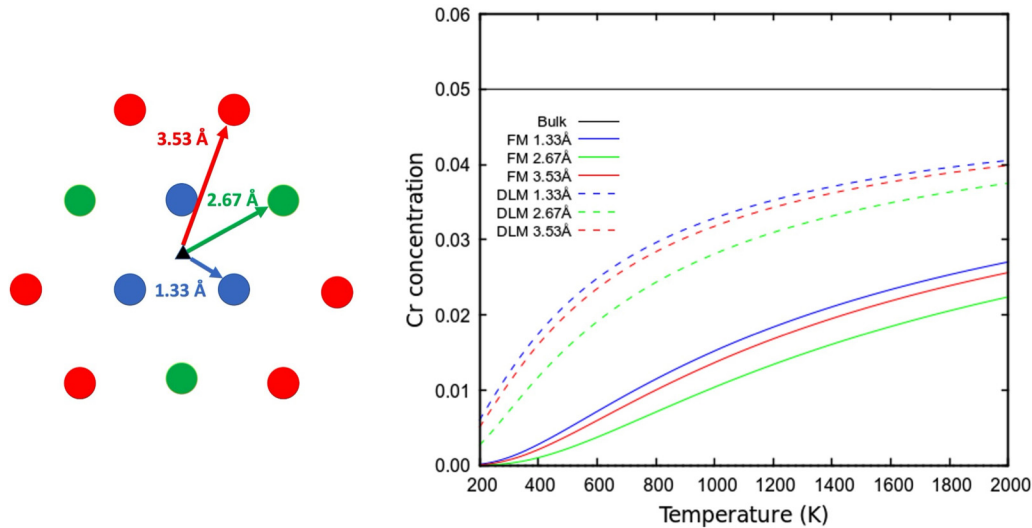


**FIG. 5.** Cr concentrations on sites closest to the dislocation core as a function of temperature using a mean-field approach. Both results from ferromagnetic and paramagnetic DLM and simulations are shown.

line. However, regardless of the magnetic state chosen in the modeling, Cr is found to, in various degrees, avoid the dislocation line. A reminiscence of this effect is seen even at 2000 K, above the experimental melting point of Fe, where the DLM modeling suggests a Cr content in the dislocation core corresponding to 80% of the bulk value.

#### IV. CONCLUSION

In this work, we have assessed the effect of disordered magnetism, modeling the paramagnetic state, on the interaction of dilute Cr solutes with  $\frac{1}{2}\langle 111 \rangle$  screw dislocation in bcc iron. We compared and contrasted this interaction between the ferromagnetic and paramagnetic states. In the FM state, Cr in both the bulk and the dislocation system wants to be as far away as possible to other Cr, in contrast with the DLM case that favors Cr clustering. The behavior of Cr solutes in the presence of a dislocation is qualitatively similar between the FM and DLM states, displaying a repulsion tendency of Cr atoms from the dislocation core. However, the extent of this repulsion is much weaker in the disordered magnetic state than in the FM state, exhibiting almost no Cr–Cr repulsion along the  $[111]$  direction, allowing for a larger presence of Cr atoms along the dislocation line in the DLM case. The segregation profile given by the mean-field approximation shows that at low temperature, Cr avoids the dislocations. With increasing temperature and connected entropic effects, Cr atoms gradually increase their occupation of dislocation sites, with around twice the amount of Cr in the DLM case than in the FM case, but still lower than the bulk limit. Although a direct comparison with experiments is difficult to establish, particularly in this idealized dislocation settings, radioactive tracers<sup>45</sup> and high temperature TEM could be a pathway to make the connection with theory. As the segregation of solutes to or away from dislocations can influence dislocation

mobility and is connected to mechanical properties, the present work highlights the importance of understanding magnetic order-disorder effects in steels and other alloys with magnetic components.

#### ACKNOWLEDGMENTS

The computations were enabled by resources provided by the Swedish National Infrastructure for Computing (SNIC) located at the National Supercomputer Centre (NSC) in Linköping, partially funded by the Swedish Research Council through Grant Agreement No. 2018-05973. B.A. acknowledges the financial support from the Swedish Research Council (VR) through Grant No. 2019-05403 from the Swedish Government Strategic Research Area in Materials Science on Functional Materials at Linköping University (Faculty Grant SFOMatLiU No. 2009-00971) and from the Knut Alice Wallenberg Foundation (Wallenberg Scholar Grant No. KAW-2018.0194), as well as the support from the Swedish Foundation for Strategic Research (SSF) through the Future Research Leaders 6 program, No. FFL 15-0290.

#### AUTHOR DECLARATIONS

##### Conflict of Interest

The authors have no conflicts to disclose.

##### Author Contributions

**Luis Casillas-Trujillo:** Conceptualization (equal); Investigation (equal); Methodology (equal); Writing – original draft (lead). **Björn Alling:** Conceptualization (equal); Funding acquisition (lead); Methodology (equal); Supervision (lead); Writing – review & editing (lead).

24 August 2023 13:41:05

## DATA AVAILABILITY

The data that support the findings of this study are available from the corresponding author upon reasonable request.

## REFERENCES

- <sup>1</sup>A. Kohyama, A. Hishinuma, D. S. Gelles, R. L. Klueh, W. Dietz, and K. Ehrlich, *J. Nucl. Mater.* **233–237**, 138 (1996).
- <sup>2</sup>F. A. Garner, M. B. Toloczko, and B. H. Sencer, *J. Nucl. Mater.* **276**, 123 (2000).
- <sup>3</sup>E. A. Little and D. A. Stow, *J. Nucl. Mater.* **87**, 25 (1979).
- <sup>4</sup>S. I. Porollo, A. M. Dvoriashin, A. N. Vorobyev, and Y. V. Konobeev, *J. Nucl. Mater.* **256**, 247 (1998).
- <sup>5</sup>L. K. Béland, Y. N. Osetsky, R. E. Stoller, and H. Xu, *J. Alloys Compd.* **640**, 219 (2015).
- <sup>6</sup>M. Itakura, H. Kaburaki, and M. Yamaguchi, *Acta Mater.* **60**, 3698 (2012).
- <sup>7</sup>K. Odbadrakh, G. Samolyuk, D. Nicholson, Y. Osetsky, R. E. Stoller, and G. M. Stocks, *Acta Mater.* **121**, 137 (2016).
- <sup>8</sup>B. Lüthi, L. Ventelon, D. Rodney, and F. Willaime, *Comput. Mater. Sci.* **148**, 21 (2018).
- <sup>9</sup>E. Clouet, L. Ventelon, and F. Willaime, *Phys. Rev. B* **84**, 224107 (2011).
- <sup>10</sup>L. Ventelon and F. Willaime, *Philos. Mag.* **90**, 1063 (2010).
- <sup>11</sup>G. Hachet, L. Ventelon, F. Willaime, and E. Clouet, *Acta Mater.* **200**, 481 (2020).
- <sup>12</sup>Y.-H. Li, H.-B. Zhou, F. Gao, G. Lu, G.-H. Lu, and F. Liu, *Acta Mater.* **226**, 117622 (2022).
- <sup>13</sup>B. Lüthi, L. Ventelon, C. Elsässer, D. Rodney, and F. Willaime, *Modell. Simul. Mater. Sci. Eng.* **25**, 084001 (2017).
- <sup>14</sup>L. Ventelon, B. Lüthi, E. Clouet, L. Provaille, B. Legrand, D. Rodney, and F. Willaime, *Phys. Rev. B* **91**, 220102 (2015).
- <sup>15</sup>E. Clouet, L. Ventelon, and F. Willaime, *Phys. Rev. Lett.* **102**, 055502 (2009).
- <sup>16</sup>D. Rodney, L. Ventelon, E. Clouet, L. Pizzagalli, and F. Willaime, *Acta Mater.* **124**, 633 (2017).
- <sup>17</sup>L. Ventelon, F. Willaime, E. Clouet, and D. Rodney, *Acta Mater.* **61**, 3973 (2013).
- <sup>18</sup>B. Alling, *Phys. Rev. B* **82**, 054408 (2010).
- <sup>19</sup>H. Landolt and R. Boernstein, *Diffusion in Solid Metals and Alloys* (Springer Berlin Heidelberg, New York, 1990).
- <sup>20</sup>H. Mehrer, *Diffusion in Solids: Fundamentals, Methods, Materials, Diffusion-Controlled Processes* (Springer Science & Business Media, 2007), Vol. 155.
- <sup>21</sup>H. Mehrer and M. Lübbehusen, *Defect and Diffusion Forum* (Trans Tech Publ, 1990), p. 591.
- <sup>22</sup>B. Bienvenu, C. C. Fu, and E. Clouet, *Acta Mater.* **200**, 570 (2020).
- <sup>23</sup>L. Hu *et al.*, *Phys. Rev. Lett.* **121**, 066401 (2018).
- <sup>24</sup>K. Odbadrakh, A. Rusanu, G. M. Stocks, G. D. Samolyuk, M. Eisenbach, Y. Wang, and D. M. Nicholson, *J. Appl. Phys.* **109**, 07E159 (2011).
- <sup>25</sup>B. Alling, T. Marten, and I. A. Abrikosov, *Nat. Mater.* **9**, 283 (2010).
- <sup>26</sup>F. Rivadulla *et al.*, *Nat. Mater.* **8**, 947 (2009).
- <sup>27</sup>D. Gambino and B. Alling, *Phys. Rev. B* **98**, 064105 (2018).
- <sup>28</sup>D. Gambino, O. I. Malyi, Z. Wang, B. Alling, and A. Zunger, *Phys. Rev. B* **106**, 134406 (2022).
- <sup>29</sup>O. Hegde, M. Grabowski, X. Zhang, O. Waseda, T. Hickel, C. Freysoldt, and J. Neugebauer, *Phys. Rev. B* **102**, 144101 (2020).
- <sup>30</sup>P. Delange, T. Ayrat, S. I. Simak, M. Ferrero, O. Parcollet, S. Biermann, and L. Pourvorskii, *Phys. Rev. B* **94**, 100102 (2016).
- <sup>31</sup>L. Casillas-Trujillo, D. Gambino, L. Ventelon, and B. Alling, *Phys. Rev. B* **102**, 094420 (2020).
- <sup>32</sup>B. L. Györfy, A. J. Pindor, J. Staunton, G. M. Stocks, and H. Winter, *J. Phys. F: Metal Phys.* **15**, 1337 (1985).
- <sup>33</sup>I. A. Abrikosov, A. V. Ponomareva, P. Steneteg, S. A. Barannikova, and B. Alling, *Curr. Opin. Solid State Mater. Sci.* **20**, 85 (2016).
- <sup>34</sup>B. Alling, T. Marten, and I. A. Abrikosov, *Phys. Rev. B* **82**, 184430 (2010).
- <sup>35</sup>E. Clouet, *Handbook of Materials Modeling: Methods: Theory and Modeling* (Springer, 2020), p. 1503.
- <sup>36</sup>E. Clouet Babel, see <http://emmanuel.clouet.free.fr/Programs/Babel> for the Babel software and documentation.
- <sup>37</sup>P. E. Blöchl, *Phys. Rev. B* **50**, 17953 (1994).
- <sup>38</sup>G. Kresse and J. Furthmüller, *Comput. Mater. Sci.* **6**, 15 (1996).
- <sup>39</sup>G. Kresse and J. Furthmüller, *Phys. Rev. B* **54**, 11169 (1996).
- <sup>40</sup>J. P. Perdew, K. Burke, and M. Ernzerhof, *Phys. Rev. Lett.* **77**, 3865 (1996).
- <sup>41</sup>P. Olsson, I. A. Abrikosov, L. Vitos, and J. Wallenius, *J. Nucl. Mater.* **321**, 84 (2003).
- <sup>42</sup>P. Olsson, I. A. Abrikosov, and J. Wallenius, *Phys. Rev. B* **73**, 104416 (2006).
- <sup>43</sup>P. M. Anderson, J. P. Hirth, and J. Lothe, *Theory of Dislocations* (Cambridge University Press, 2017).
- <sup>44</sup>G. Tréglia, B. Legrand, F. Ducastelle, A. Saúl, C. Gallis, I. Meunier, C. Mottet, and A. Senhaji, *Comput. Mater. Sci.* **15**, 196 (1999).
- <sup>45</sup>C.-G. Lee, Y. Iijima, T. Hiratani, and K.-I. Hirano, *Mater. Trans. JIM* **31**, 255 (1990).